Supplementary Materials

Title: Disrupting the LINC Complex in Smooth Muscle Cells Reduces Aortic Disease in a Mouse Model of HGPS

Authors: Paul Kim, Jennings Luu, Patrick Heizer, Yiping Tu, Thomas A. Weston, Natalie Chen, Christopher Lim, Robert L. Li, Po-Yu Lin, James C. Y. Dunn, Didier Hodzic, Stephen G. Young, and Loren G. Fong

Materials and Methods

Fig. S1. Pathology in *Lmna*^{G609G} mice.

Fig. S2. Absence of fibrosis in aortas of young mice and non-aortic tissues of *Lmna*$^{G609G/+}$ mice.

Fig. S3. Abnormal cell and nuclear cell morphology in *Lmna*^{G609G} aortic smooth muscle cells.

Fig. S4. Progerin is expressed at high levels in the aorta of *Lmna*$^{G609G/+}$ mice.

Fig. S5. Aortic pathology is more severe at the inner curvature of the ascending aorta in *Lmna*$^{G609G/G609G}$ mice.

Fig. S6. Control studies for the lamin-inducible smooth muscle cell (SMC) system and the *Sm22-Cre*–dependent activation of KASH2 expression in the aorta.

Table S1. Antibodies used for western blotting and immunohistochemistry.

Table S2. Quantitative RT-PCR primers.

Materials and Methods

Mice. *Zmpste24*$^{-/-}$ and *Lmna*$^{G609G/G609G}$ mice have been described previously (*38, 67*). Sm22α-*Cre* transgenic (stock no. 017491) and mT/mG reporter (stock no. 007676) mice were purchased from The Jackson Laboratory (Bar Harbor, ME). The Sm22α-*Cre* mouse strain was genotyped by PCR with forward primer 5′-CAGACACCGAAGCTACTCTCCTTCC-3′ and reverse primer 5′-CGCATAACCAGTGAAACAGCATTGC-3′ (yielding a 500-bp product). The mT/mG mouse strain was genotyped with a mutant forward primer 5′-TAGAGCTTGCGGAACCCTTC-3′, a wild-type forward primer 5′-AGGGAGCTGCAGTGGAGTAG-3′, and a common reverse primer 5′-CTTTAAGCCTGCCCAGAAGA-3′ (128-bp product for the mutant allele; 212-bp product for the wild-type allele). The CAG-LacZ/EGFP-KASH2 transgenic mouse (*51*) was genotyped with forward primer 5′-GGAGTTCGTGACCGCCGCCGGGATCACTCT-3′ and reverse primer 5′-TTTAAACGGGCCCCCTAGGTGGGAGGTGGC-3′ (yielding a ~280-bp product). Mice were housed in a specific pathogen–free barrier facility with a 12-h light/dark cycle. The mice were provided pelleted mouse chow (NIH31) and water *ad libitum* and nutritional food cups (Westbrook, ME) as required for supportive care. All animal studies were approved by UCLA's Animal Research Committee.

Cells. Immortalized mouse aortic smooth muscle cells (#CRL-2797) were purchased from the American Type Culture Collection (Manassas, VA) and cultured in DMEM (Gibco; Gaithersburg, MD) containing 10% FBS (Hyclone), 1× nonessential amino acids (Gibco), 1 mM sodium pyruvate (Gibco), 2 mM glutamine (Gibco), and 0.2 mg/ml G418 (Gibco). The cells exhibit both synthetic and contractile phenotypes, as judged by a high proliferation rate and absence of smooth muscle myosin heavy chain expression (*68*), and perinuclear distribution of

vimentin (*69*), respectively. The cells were transduced with lentivirus by UCLA's Vector Core Facility. To produce UV-treated cells, SMCs in 6-well dishes were exposed to 100mJ/cm2 UV light in a Stratalinker 2400 (Stratagene; La Jolla, CA). Cells were transfected with 100 nM *Lmnb1* siRNA (AM16706; Ambion) using RNAiMAX (Invitrogen) according to manufacturer's instructions.

pTRIPZ-Prelamin A and pTRIPZ-progerin lentiviral vectors. A human prelamin A cDNA in pCMV-XL5 vector (#SC101048) was purchased from Origene (Rockville, MD). A human progerin cDNA was created by deleting 150 nucleotides (1818–1968) from the prelamin A cDNA with the QuikChange Lightening kit (Agilent; Santa Clara, CA) and mutagenic primers (forward primer, 5′-GCTCAGGAGCCCAGAGCCCCCAGAACTG-3′; reverse primer, 5′-CAGTTCTGGGGGCTCTGGGCTCCTGAGC-3′). The doxycycline-inducible vector pTRIPZ-hDDX5/17 (Addgene; Cambridge, MA) was digested with restriction enzymes *Age*I and *Eco*RI to delete the red fluorescence protein and shRNA sequences and then gel-purified. The human prelamin A and progerin cDNAs were amplified with the Titanium Taq PCR kit (Clontech; Mountain View, CA) and sequence-specific primers (forward primer, 5′-GTCAGATCGCACCGGATGGAGACCCCGTCCCAG-3′; and reverse primer, 5′-GTAGCCCCTTGAATTTTACATGATGCTGCAGTTCTGGGG-3′). The fragments were purified with UltraClean15 (Mo-bio) and subcloned into the prepared pTRIPZ vector with In-Fusion Cloning (Clontech). The products were amplified in XL10-Gold Ultracompetent cells (Agilent) and plasmids with the correct sequence were isolated with plasmid kits (Qiagen; Germantown, MD). Packaging of lentivirus and transduction of cells were performed by UCLA's Vector Core. Transduced cells were selected for two weeks with 1.5 μg/ml puromycin.

pLenti6-EGFP-KASH2 and pLenti6-EGFP-KASHext lentiviral vectors. The EGFP-KASH2 sequence was amplified from pEGFP-C1-KASH2 (*50*) with the TaKaRa LA PCR kit (Clontech) and sequence-specific primers (forward primer, 5′-ACACCGACTCTAGAGATGGTGAGCAAGGGCGAGGA-3′; and reverse primer, 5′-GCGGGCCCTCTAGACCTAGGTGGGAGGTGGCCCGT-3′). The EGFP-KASHext sequence was amplified from pEGFP-C1-KASHext (*50*) with the TaKaRa LA PCR kit (Clontech) and sequence-specific primers (forward primer, 5′-ACACCGACTCTAGAGATGGTGAGCAAGGGCGAGGA-3′; and reverse primer, 5′-GCGGGCCCTCTAGACTTATCTAGATCCGGTGGATC-3′). The gel-purified fragments were subcloned into the pLenti6/v5-DEST plasmid (ThermoFisher) (linearized with *Bam*HI and *Xho*I), with In-Fusion Cloning (Clontech). The products were amplified in XL10-Gold Ultracompetent cells (Agilent) and plasmids with the correct sequences were isolated with plasmid kits (Qiagen; Germantown, MD). Packaging of lentivirus and transduction of pTRIPZ-prelamin A or pTRIPZ-progerin cells were performed by UCLA's Vector Core. Transduced cells were selected for two weeks with 2 μg/ml blasticidin.

Stretching smooth muscle cells on polydimethylsiloxane (PDMS) membranes. Flexible PDMS membranes (1-mm-thick) were prepared in 150-mm culture dishes with the Sylgard 184 silicone elastomer kit (Dow-Corning #3097358-1004). Membranes strips (7 × 0.8 cm) were activated with a plasma cleaner, treated with 2% 3-aminopropy-triethoxysilane at RT for 45 min, washed in ethanol, and then dried at 55° C for 30 min. The membranes were incubated with 0.5 mg/ml sulfo-SANPAH in HEPES buffer and crosslinked with UV exposure (300–460 nm) for 30 sec. The washed membranes were stored at 4° C in a 100 μg/ml collagen solution (PureCol 5005; Advanced Biomatrix). Cells (1×10^5) were added to individual membrane strips in molds and

incubated in media ± doxycycline for 24 h and then clamped into a custom-built stretching device. The brackets holding the membranes were attached to an L12 linear actuator (Actuonix; Victoria, Canada) controlled by a multifunction DAQ device (National Instruments; Austin, TX) and LabVIEW 2015 software (National Instruments). The membranes were stretched 6-mm at 0.5 Hz (24 h) for the cell-viability studies (trypan blue and cell protein measurements), 3-mm at 0.5 Hz (24 h) for the DNA-damage studies (western blotting studies), and 2-mm at 0.5 Hz (2 h) for the cell-damage studies (propidium iodide studies). The milder conditions for the DNA- and cell-damage studies were to examine the effects of mechanical stress prior to cell death. To measure cell protein, membranes were washed with PBS, digested with 0.1 N NaOH, and protein content measured with the D-C protein assay kit (BioRad; Richmond, CA). To stain cells with propidium iodide (PI), membranes were incubated with freshly prepared 10 μg/ml PI (ThermoFisher) and 1 μg/ml Hoechst 33342 (ThermoFisher) in Dulbecco's PBS at RT for 15-min. The stained cells were washed, fixed, and analyzed by fluorescence microscopy.

Separation of aortic adventitia and media layers. The adventitia and media layers of the mouse aorta were separated by enzymatic digestion (*44*). Cleaned aortas were incubated in PBS containing 1 mg/ml collagenase type II, 1 mg/ml soybean trypsin inhibitor, and 2 mg/ml elastase (all from Worthington; Lakewood, NJ) at 37° C for 10 min. The digested aortas were placed into ice-cold PBS, cut into three segments of equal length, and the adventitia layer unrolled from each segment. The adventitia and media (also including the endothelial cell layer) were processed immediately or frozen in liquid nitrogen for storage.

Western blotting. Urea-soluble protein extracts from cells and tissues were prepared as described (*38*). Proteins were size-fractionated on 4–12% gradient polyacrylamide Bis-Tris gels (Invitrogen) and transferred to nitrocellulose membranes. The membranes were blocked with

Odyssey Blocking solution (LI-COR Bioscience, Lincoln, NE) for 1 h at RT and incubated with primary antibodies at 4° C overnight. After washing the membranes with PBS containing 0.2% Tween-20, they were incubated with infrared dye (IR)–labeled secondary antibodies at RT for 1 h. The IR signals were quantified with an Odyssey infrared scanner (LI-COR Biosciences). The antibodies and concentrations are listed in Table S1.

Immunofluorescence microscopy. Cells on coverslips or tissue sections (6–10-μm-thick) on glass slides were fixed with 4% paraformaldehyde in PBS and permeabilized with 0.2% Triton. The cells were processed for immunofluorescence microscopy as described (*70, 71*). The antibodies and concentrations are listed in Table S1. Confocal fluorescence microscopy images were obtained with a Zeiss LSM700 laser–scanning microscope and images along the *z*-axis were processed by Zen 2010 software (Zeiss) to generate maximum image projections. Nuclear shape abnormalities in cells were scored by two independent trained observers blinded to genotype (*70, 71*). A minimum of 200 cells were scored for each group.

Histological analysis. Mice were perfused *in situ* with PBS followed by fixative solution (3% paraformaldehyde in PBS). The entire thoracic aorta was dissected free and incubated in fixative solution for 24–48 h at 4° C. Aortic rings (~2-mm-long) from the proximal ascending aorta, mid-arch, proximal descending, and mid-descending aorta were embedded in paraffin, and sections (4–6-μm) were stained with hematoxylin and eosin (HNE), Masson's trichrome, or Verhoeff-Van Gieson stain by UCLA's Translational Pathology Core Laboratory. The stained sections were coded, and photographs captured on a Nikon E600 light microscope with 20× and 40× objectives with a Nikon DS-Fi2 camera operated by NIS Elements software (Version 4.0). The images (tiff format) were imported into ImageJ1.50i, and the areas of the media and adventitia were measured. The number of nuclei in the media were counted and expressed as #nuclei/media

area. Adventitial area was expressed as a percentage of total area [adventitia area/(adventitia area + media area)].

Quantitative real time-PCR. Total RNA was isolated and treated with DNase I (Ambion, Life Technologies). RNA was reverse-transcribed with random primers, oligo(dT), and SuperScript III (Invitrogen). qPCR reactions were performed on a 7900HT Fast Real-Time PCR system (Applied Biosystems) with SYBR Green PCR Master Mix (Bioline, Taunton, MA). Transcript levels were determined by the comparative cycle threshold method and normalized to levels of cyclophilin A. Primer sequences are listed in Table S2.

Electron microscopy. Mice were perfused *in situ* with PBS followed by ice-cold fixative (3% paraformaldehyde in PBS). Aortic samples were incubated overnight in glutaraldehyde fixative solution containing 2.5% glutaraldehyde (EMS; Hatfield, PA), 4% paraformaldehyde (EMS), 2.1% sucrose (Sigma; Burlington, MA) and buffered with 0.1 M sodium cacodylate (Sigma). The following day, tissues were rinsed three times with 0.1 M sodium cacodylate and fixed with 2% osmium tetroxide (EMS) buffered with 0.1 M sodium cacodylate at RT for 1 h. The samples were rinsed three times with distilled water and stained overnight with 2% uranyl acetate at 4° C. The samples were rinsed three times with distilled water and dehydrated with increasing concentrations of acetone (30%, 50%, 70%, 85%, 95%, 100%; 3 × 10 min each) before infiltration with Spurr's epoxy resin (EMS) in acetone (33% for 2 h; 66% overnight; 100% for 4 h). The samples were flat-embedded in caps of BEEM capsules (EMS) and polymerized in a vacuum oven at 65° C for 24 h. The polymerized "pucks" were removed from the caps and glued onto the tops of polymerized BEEM capsules for trimming and sectioning. Sections (65-nm) were cut on a Leica UC6 ultramicrotome and picked up on freshly glow-discharged copper grids (Ted Pella; Redding, CA) that were coated with formvar and carbon. Sections on grids were then

stained with Reynold's lead citrate solution for 10 min. Images were acquired with an FEI T12 transmission electron microscope set to 120 kV accelerating voltage and a Gatan 2K × 2K digital camera (Electron Imaging Center) or with a JEOL 100CX electron microscope set at 60 kV on type 4489 EM film (BRI Electron Microscopy Core Facility). Film negatives were scanned to create digital files.

Statistical analysis. Statistical analyses were performed with Microsoft Excel for Mac 2011 and GraphPad software. Experimental groups were analyzed by a two-tailed Student's *t*-test.

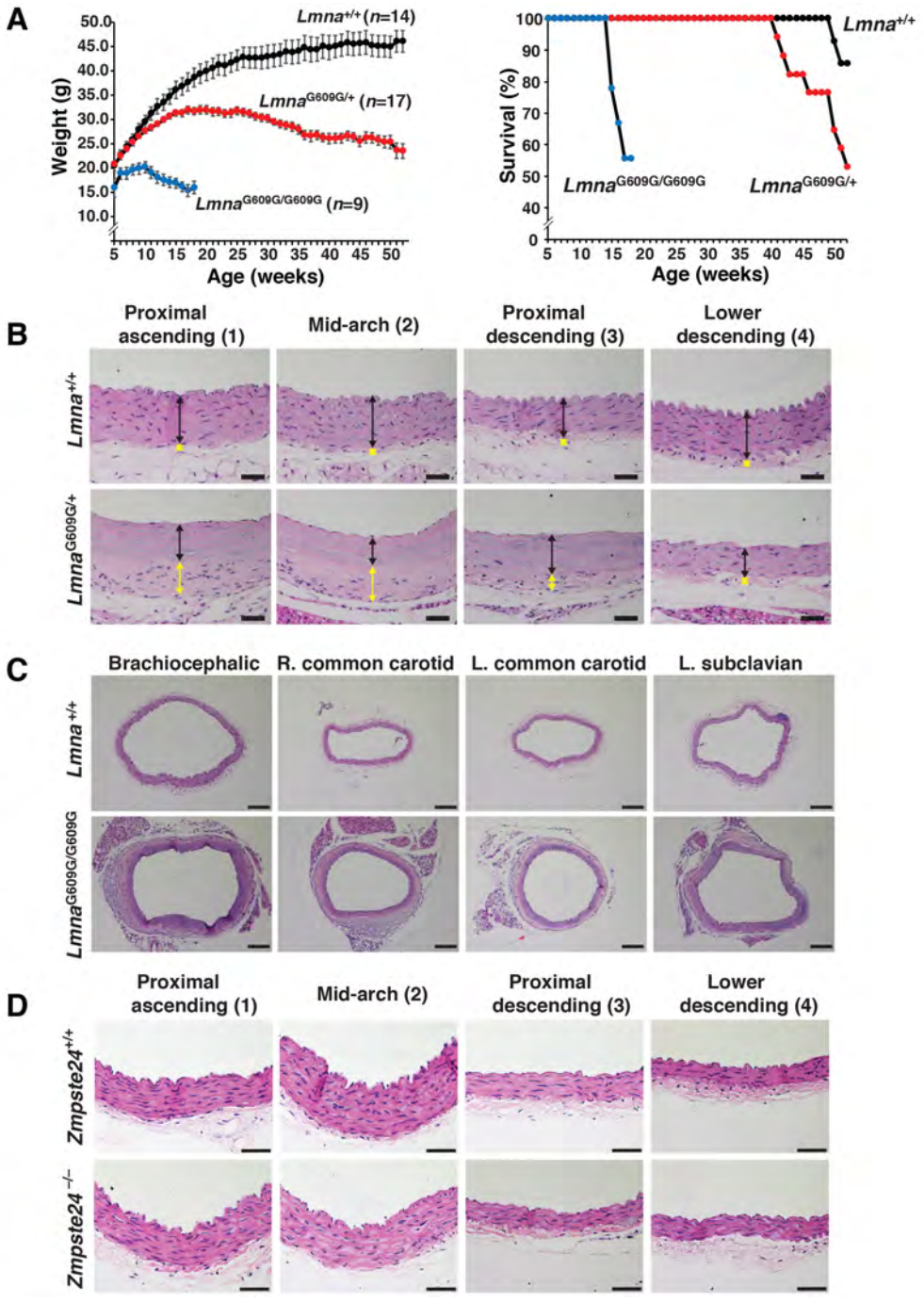

Figure S1. Pathology in *Lmna*^{G609G} mice. (a) Body weight gain and survival curves for *Lmna*$^{+/+}$ (black line; n = 14), *Lmna*$^{G609G/+}$ (red line; n = 17), and *Lmna*$^{G609G/G609G}$ (blue line; n = 9) mice. (b) HNE-stained sections of different regions of the aorta in 12-month old *Lmna*$^{+/+}$ and *Lmna*$^{G609G/+}$ mice (proximal ascending, mid-arch, proximal descending, and lower descending). Colored lines identify the media (black) and adventitia (yellow). Scale bar, 20 µm. (c) HNE-

stained sections of the brachiocephalic artery, right (R) common carotid, left (L) common carotid, and L. subclavian artery from 4.5-month-old *Lmna*$^{+/+}$ and *Lmna*$^{G609G/G609G}$ mice. Scale bar, 100 μm. (d) HNE-stained sections of the same regions described in panel b, but collected from 4.5-month-old *Zmpste24*$^{+/+}$ and *Zmpste24*$^{-/-}$ mice. Scale bar, 50 μm.

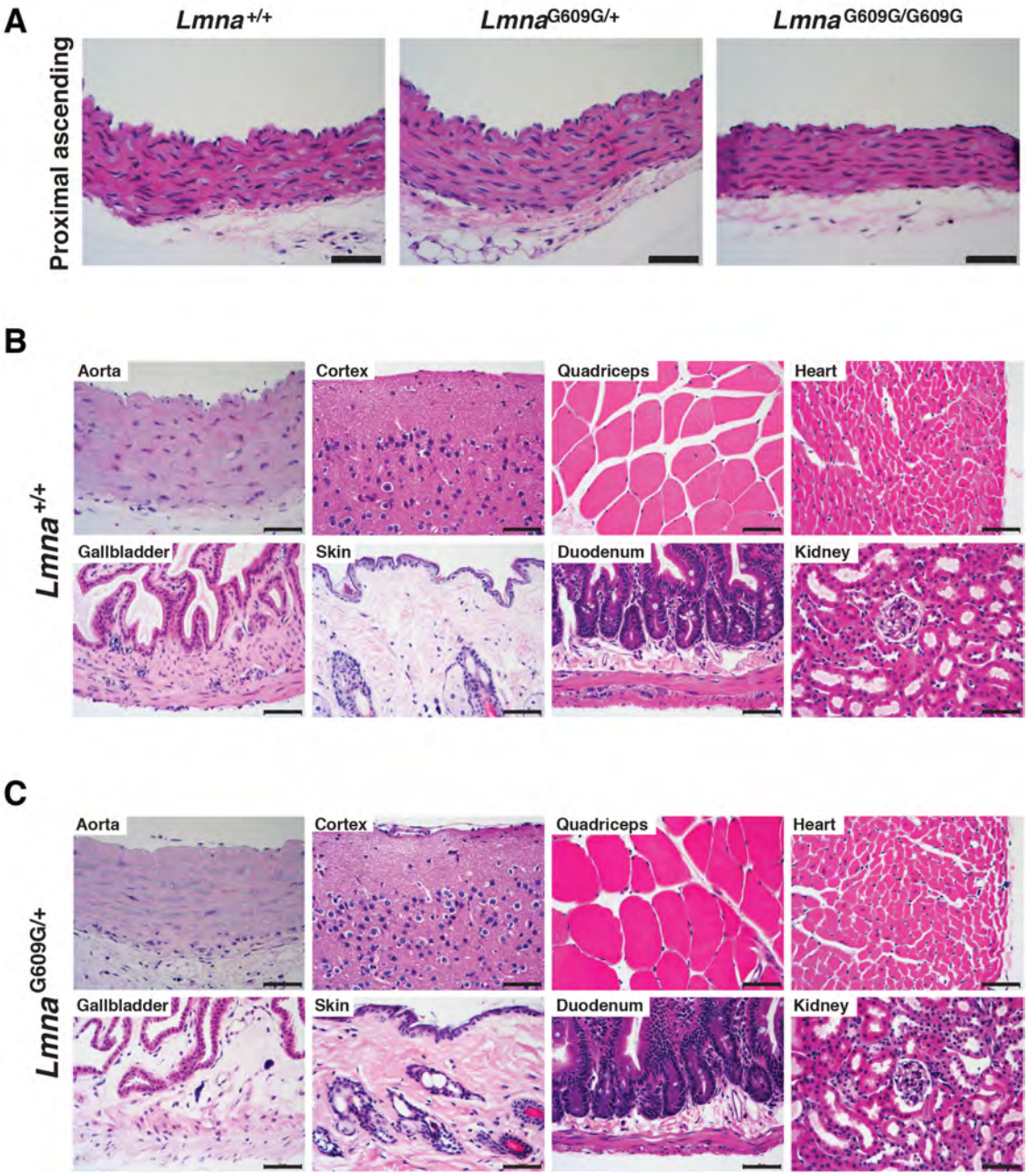

Figure S2. Absence of fibrosis in aortas of young mice and non-aortic tissues of *Lmna*$^{G609G/+}$ mice. (a) HNE-stained sections of the proximal ascending aorta from 2-month-old wild-type, *Lmna*$^{G609G/+}$, and *Lmna*$^{G609G/G609G}$ mice. Scale bar, 50 µm. (b–c) HNE-stained sections of the proximal ascending aorta, cerebral cortex, quadriceps, heart, gallbladder, skin, duodenum, and kidney from 12-month-old wild-type (b) and *Lmna*$^{G609G/+}$ (c) mice. Scale bar, 50 µm.

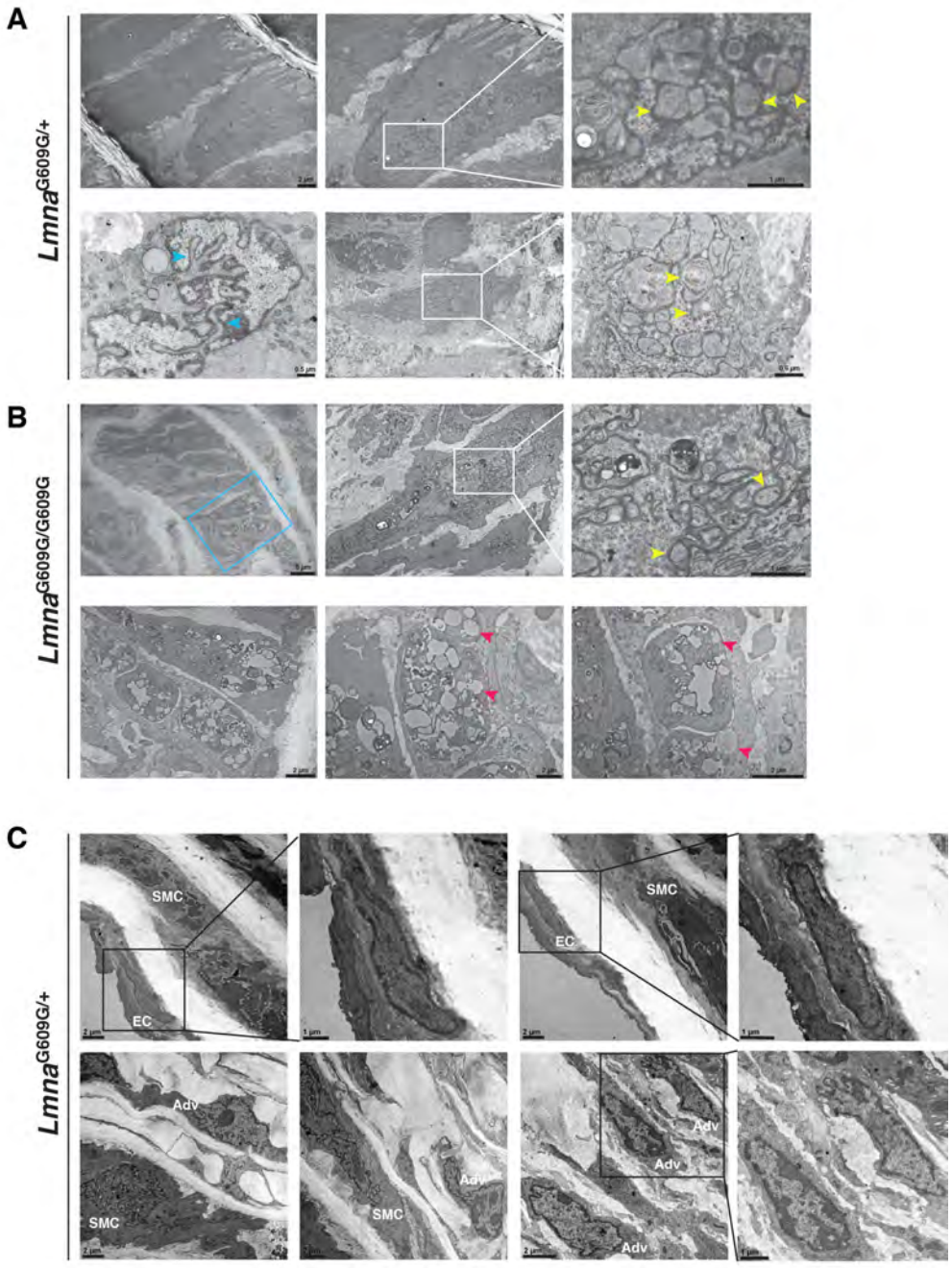

Figure S3. Abnormal cell and nuclear cell morphology in *Lmna*^{G609G} aortic smooth muscle cells. Cell morphology in the thoracic aorta was examined by transmission electron microscopy. (a) Low- and high-magnification images of smooth muscle cells (SMCs) from 9-month-old *Lmna*$^{G609G/+}$ mice. The boxed areas in the middle panels are shown at higher magnification in images to the right. Yellow arrowheads point to intranuclear vesicles, some with cytoplasmic

organelles. Blue arrowheads point to intranuclear tubules. (b) Low- and high-magnification images of SMCs from a 3-month-old *Lmna*$^{G609G/G609G}$ mouse. The blue-colored box is shown at higher magnification in the lower panels. The white-colored box in the middle panel is shown at higher magnification in the image to the right. Yellow arrowheads point to intranuclear vesicles, and red arrowheads point to cytoplasmic vacuoles. (c) Low- and high-magnification images of endothelial cells (EC) (upper row) and adventitial cells (Adv) (lower row) from a 3-month-old *Lmna*$^{G609G/G609G}$ mouse. The black-colored boxes are shown at higher magnification in images to the right. Scale bars are shown in the images.

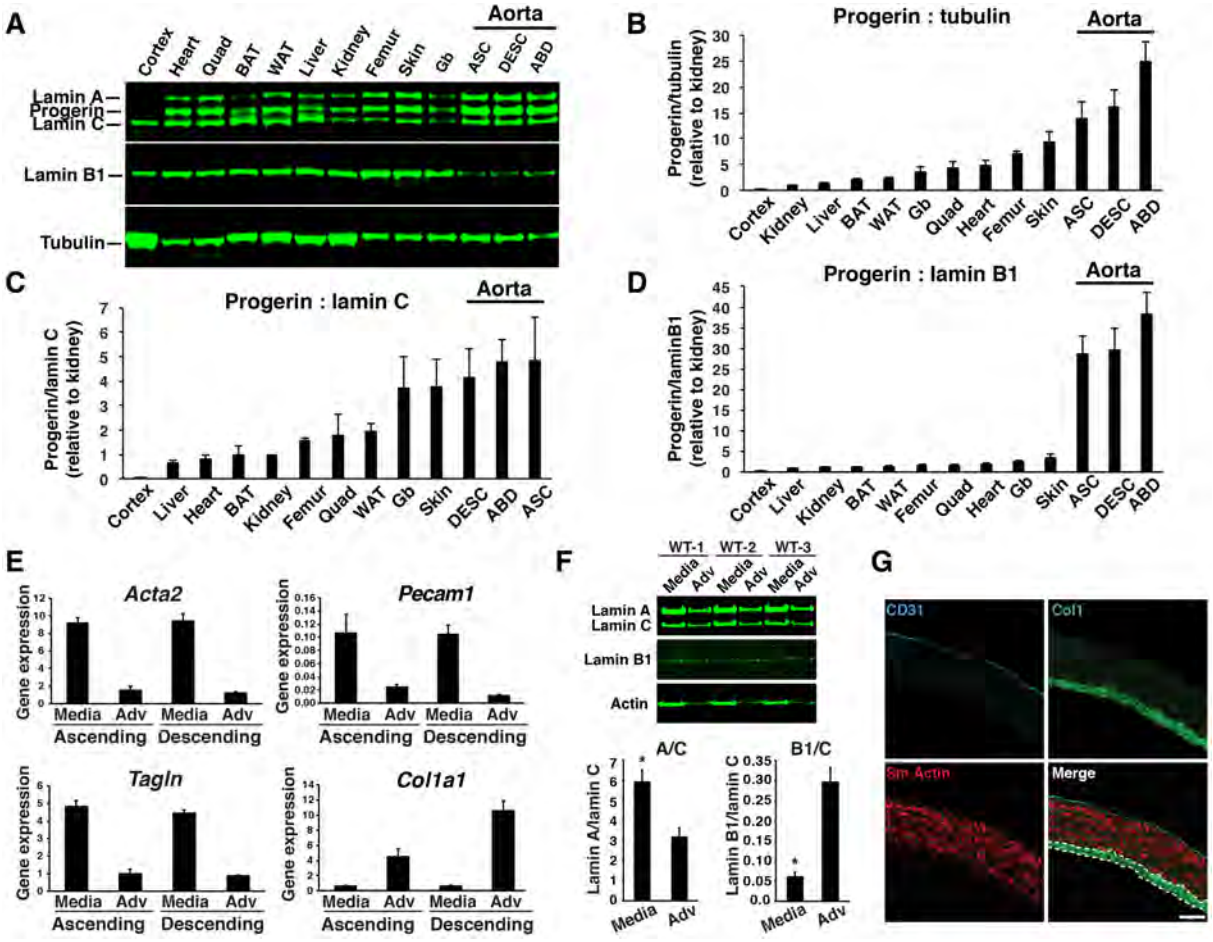

Figure S4. Progerin is expressed at high levels in the aorta of *Lmna*$^{G609G/+}$ mice. The expression of nuclear lamins in different tissues of *Lmna*$^{G609G/+}$ mice was measured by western blotting. (a) Representative western blot comparing the expression of lamin A, progerin, lamin C, and lamin B1 in different tissues. Tubulin was measured as a loading control. Cortex, cerebral cortex; BAT, brown adipose tissue; WAT, white adipose tissue; Gb, gallbladder; ASC, ascending aorta; DESC, descending aorta; ABD, abdominal aorta. (b) Graph showing progerin expression relative to tubulin. (c) Graph showing progerin expression relative to lamin C. (d) Graph showing progerin expression relative to lamin B1. For panels b–d, tissues are arranged in ascending order from left to right with expression in kidney set at a value of one (mean ± SEM; *n*

= 3 mice). (e) Gene-expression studies to validate the isolation of the media and adventitial (Adv) layers (mean ± SEM; n = 4 mice). *Acta2* and *Tagln* were measured to identify SMCs; *Pecam1* for endothelial cells; and *Col1a1* for adventitial cells. (f) Western blot comparing the expression of lamin A, lamin C, and lamin B1 in the media and adventitia (Adv) in wild-type mice. Bar graphs show the expression of lamin A (left) and lamin B1 (right) relative to lamin C (mean ± SEM; n = 3). Media *vs*. adventitia; $*p < 0.03$. (g) Confocal fluorescence microscopy to identify endothelial cells, smooth muscle cells, and adventitia with antibodies against CD31 (cyan), smooth muscle cell actin (red), and collagen type I (green), respectively. In the merged image, the adventitia is outlined by dotted white lines. Scale bar, 50 μm.

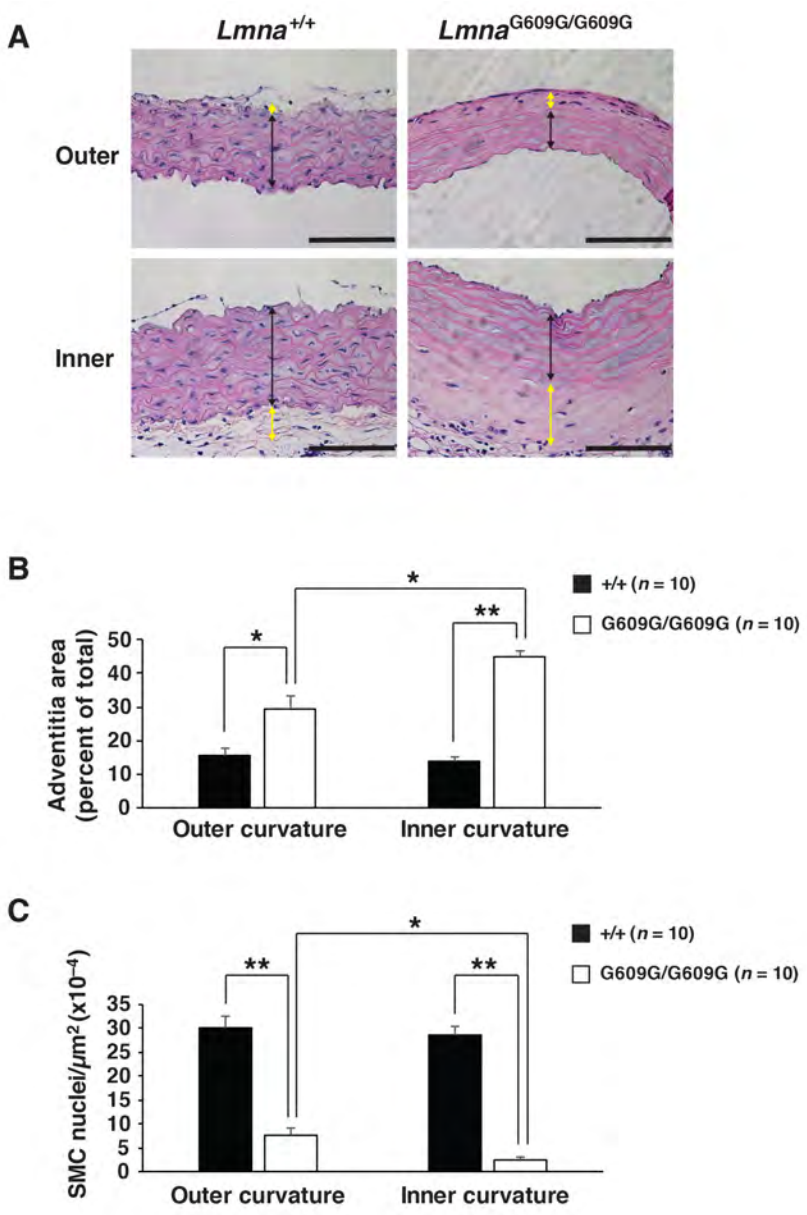

Figure S5. Aortic pathology is more severe at the inner curvature of the ascending aorta in *Lmna*$^{G609G/G609G}$ mice. The number of SMC nuclei and adventitial area were quantified at the inner and outer curvature of the ascending thoracic aorta in 4-month-old *Lmna*$^{G609G/G609G}$ mice. The white line in figure 4C shows the location where the measurements were made. (a) Representative HNE-stained sections of the inner and outer curvature of the ascending aorta in *Lmna*$^{+/+}$ and *Lmna*$^{G609G/G609G}$ mice. Colored lines identify the media (black) and adventitia (yellow). Scale bar, 100 μm. (b) Bar graph showing adventitial area (as a percentage of total

area) in wild-type (black) and *Lmna*$^{G609G/G609G}$ (white) mice at the outer and inner curvature of the ascending aorta. (c) Bar graph showing the number of SMC nuclei (relative to media area) in wild-type (black) and *Lmna*$^{G609G/G609G}$ (white) mice at the outer and inner curvature of the ascending aorta. Mean ± SEM for wild-type (n = 10) and *Lmna*$^{G609G/G609G}$ (n = 10) mice. *Lmna*$^{G609G/G609G}$ *vs*. wild-type; *$p < 0.01$ and **$p < 0.001$. (Results for the inner curvature were reported in figure 1e.)

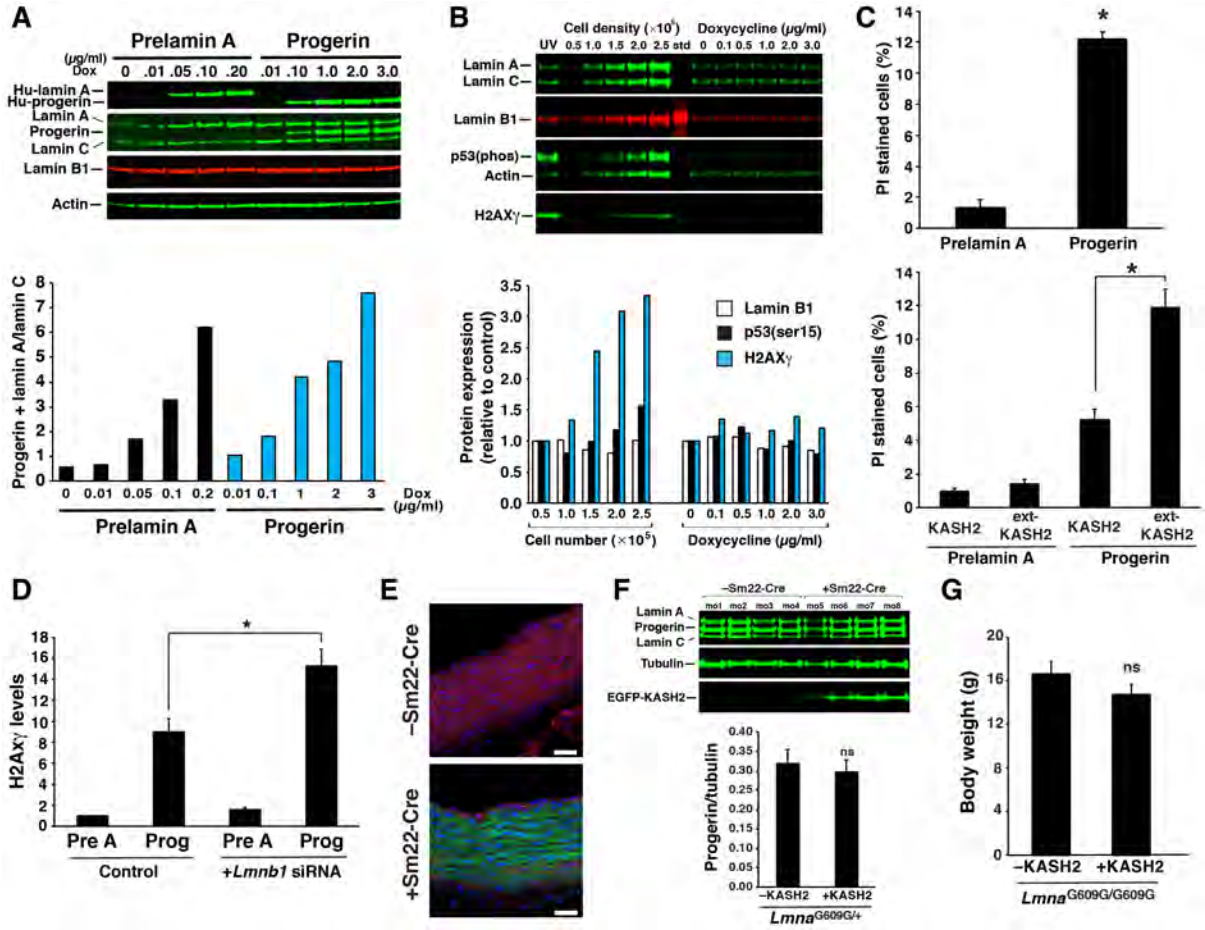

Figure S6. Control studies for the lamin-inducible smooth muscle cell (SMC) system and the *Sm22-Cre*–dependent activation of KASH2 expression in the aorta. (a) Western blot showing the dose-dependent increase in human lamin A and progerin expression in cells treated with doxycycline for 1-day. Lamin A and progerin were detected by western blot with an antibody specific for human lamin A (top panel). Total A-type lamins (lamin A, progerin, and lamin C) were measured with an antibody that recognizes both human and mouse lamin A/C (middle panel). The bar graph shows the amount of lamin A or progerin, relative to lamin C. (b) Western blots showing that H2AX-γ expression is induced by high cell density but not by doxycycline. The bar graph shows the expression of lamin B1 (white), phos-p53 (black), and H2AX-γ (blue), relative to actin and normalized to either the 0.5×10^5 group or the no-

doxycycline group (both set at a value of one). (c) Upper bar graph shows increased propidium iodide (PI) staining in progerin-expressing cells as compared to prelamin A-expressing cells after stretching for 2 h at 0.5 Hz (2-mm). The mean ± SEM (n = 3 experiments) is shown. Lower bar graph shows KASH2 expression reduces PI staining in stretched progerin-expressing cells. Cells expressing the inactive KASH2 mutant (ext-KASH2) is included as a control. The mean ± SEM (n = 3 experiments) is shown. *, $p < 0.05$. (d) Reducing lamin B1 levels increase H2AX-γ expression in progerin (Prog)-expressing cells. All cells were exposed to repetitive stretching (2-mm at 0.5Hz) for 2 h. SiRNA treatment reduced lamin B1 protein levels by 45% (n = 3). The bar graph shows H2AX-γ levels relative to control-treated prelamin A (Pre A)–expressing cells. The mean ± SEM (n = 3 experiments) is shown. Control *vs*. *Lmnb1* siRNA-treated; *$p < 0.05$. (e) The expression pattern for the *Sm22-Cre* transgene was examined by intercrossing *Sm22-Cre* transgenic mice with the mT/mG reporter mouse. *Cre*-mediated recombination was identified by EGFP fluorescence (green). Scale bar, 20 μm. (f) Western blotting showing that KASH2–EGFP expression in SMCs (+Sm22-Cre) does not affect progerin levels in the aorta of *Lmna*$^{G609G/+}$ mice. The KASH2–EGFP fusion protein was detected with an antibody against GFP. Tubulin was used as a loading control. mo, mouse. Bar graph shows progerin levels (relative to tubulin). The mean ± SEM (n = 4 mice/group) is shown. ns (nonsignificant), $p > 0.10$. (g) Bar graph shows KASH2 expression in SMCs does not affect body weight of *Lmna*$^{G609G/G609G}$ mice at 16-weeks of age. The mean ± SEM (n = 6 mice/group) is shown. ns, $p > 0.10$.

Table S1. Antibodies used for western blotting and immunohistochemistry.

Antibody Description	Species	Source	Catalog #	Use	Dilution
β-actin	Rabbit	Abcam	ab8227	WB, IF	1:3000
β-actin	Goat	Santa Cruz Biotech	SC1616	WB, IF	1:3000
CD31	Rat	BD Pharmingen	553370	IF	1:100
Collagen type I	Rabbit	Abcam	ab21286	IF	1:200
Collagen type III	Rabbit	Abcam	ab7778	IF	1:100
Collagen type IV	Rabbit	BioRad	2150-1470	IF	1:100
Collagen type V	Rabbit	Abcam	ab7046	IF	1:100
Collagen type VIII	Rabbit	Antibodies-online	ABIN1718654	IF	1:20
GFP	Rabbit	ThermoFisher	A11122	WB, IF	1:1000
GFP	Chicken	Aves Lab	GFP1020	WB, IF	1:1000
Human lamin A	Mouse	Millipore	MAB3211	WB, IF	1:1500
Lamin A/C	Goat	Santa Cruz Biotech	SC6215S	WB, IF	1:1000
Lamin A/C	Mouse	Santa Cruz Biotech	SC376248	WB, IF	1:1500
Lamin B1	Goat	Santa Cruz Biotech	SC6217	WB, IF	1:1500

LAP2β	Mouse	BD Pharmingen	611000	IF	1:2000
Nesprin2	Rabbit	In-house	Not applicable	IF	1:1000
Phospho-H2AX	Mouse	Millipore	05-636	WB, IF	1:3000
p53(Ser15)	Rabbit	Cell Signaling Technology	9284	WB, IF	1:3000
Prelamin A (3C8)	Rat	In-house	Not applicable	WB	2 μg/ml
Sm-actin	Goat	Sigma	SAB2500963	IF	1:100
SUN1	Rabbit	Abcam	ab103021	WB, IF	1:1000
SUN1	Rabbit	Novus Bio	NBP1-87396	WB, IF	1:1000
SUN1	Mouse	Millipore	MABT892	WB, IF	1:1000
Tubulin	Rat	Novus Bio	NB600-506	WB	1:3000
Anti-rabbit IR800	Donkey	LI-COR	926-32213	WB	1:10000
Anti-goat IR800	Donkey	LI-COR	926-32214	WB	1:10000
Anti-rat IR800	Donkey	ThermoFisher	SA5-10032	WB	1:5000
Anti-mouse IR800	Donkey	ThermoFisher	SA5-10172	WB	1:5000
Anti-rabbit IR680	Donkey	LI-COR	926-32221	WB	1:5000
Anti-rat IR680	Goat	LI-COR	925-68076	WB	1:5000
Anti-chicken IR800	Goat	Rockland	603-131-126	WB	1:5000
Anti-chicken Alexa 488	Goat	Invitrogen	A11039	IF	1:2000
Anti-mouse Alexa 488	Donkey	Invitrogen	A21202	IF	1:2000

Anti-rabbit Alexa 488	Donkey	Invitrogen	A21206	IF	1:2000
Anti-goat Alexa 488	Donkey	Invitrogen	A11055	IF	1:2000
Anti-goat Alexa 555	Donkey	Invitrogen	A21432	IF	1:2000
Anti-rabbit Alexa 555	Donkey	Invitrogen	A31572	IF	1:200
Anti-rabbit Alexa 568	Donkey	Invitrogen	A10042	IF	1:2000
Anti-mouse Alexa 568	Donkey	Invitrogen	A10037	IF	1:2000
Anti-mouse Alexa 647	Donkey	Invitrogen	A31571	IF	1:2000
Anti-rabbit Alexa 647	Donkey	Invitrogen	A31573	IF	1:2000
Anti-goat Alexa 647	Donkey	Invitrogen	A21447	IF	1:2000
Anti-rat Alexa 650	Donkey	ThermoFisher	SA5-10029	IF	1:200

Table S2. Quantitative RT-PCR primers.

Gene	Forward	Reverse
Col1a1	TGACTGGAAGAGCGGAGAGT	GACGGCTGAGTAGGGAACAC
Col3a1	GACCAAAAGGTGATGCTGGACAG	CAAGACCTCGTGCTCCAGTTAG
Col4a1	ATGGCTTGCCTGGAGAGATAGG	TGGTTGCCCTTTGAGTCCTGGA
Col5a1	AGATGGCATCCGAGGTCTGAAG	GACCTTCAGGACCATCTTCTCC
Col8a1	GCTGCTGGGAATACTGTTCA	GGGTAGGTGTGGGTACTCTTT
Acta2	TCCCTGGAGAAGAGCTACGAACT	GATGCCCGCTGACTCCAT
Prelamin A	GGTTGAGGACAATGAGGATGA	TGAGCGCAGGTTGTACTCAG
Lmnb1	CAACTGACCTCATCTGGAAGAAC	TGAAGACTGTGCTTCTCTGAGC
Pecam1	CCTCAGTCGGCAGACAAGAT	ATGGATGCTGTTGATGGTGA
Tagln	CCGAAGCTACTCTCCTTCCA	GACTGCACTTCTCGGCTCAT
Lamin C	GACAATGAGGATGACGACGAG	TTAATGAAAAGACTTTGGCATGG
Ppia	TGAGCACTGGAGAGAAAGGA	CCATTATGGCGTGTAAAGTCA